PHOTONICS Research

Widely tunable passively Q-switched Er^{3+}-doped ZrF_4 fiber laser in the range of 3.4–3.7 μm based on a Fe^{2+}:ZnSe crystal

Hongyu Luo, Jian Yang, Jianfeng Li,* and Yong Liu

State Key Laboratory of Electronic Thin Films and Integrated Devices, School of Optoelectronic Science and Engineering, University of Electronic Science and Technology of China (UESTC), Chengdu 610054, China
**Corresponding author: lijianfeng@uestc.edu.cn*

Received 24 June 2019; revised 19 July 2019; accepted 23 July 2019; posted 24 July 2019 (Doc. ID 370921); published 28 August 2019

We report the first (to the best of our knowledge) tunable passively *Q*-switched Er^{3+}-doped ZrF_4 fiber laser around 3.5 μm. In this case, a Fe^{2+}:ZnSe crystal is used as the saturable absorber, and a plane-ruled grating in a Littrow configuration acts as the tuning element. At the tuned wavelength of 3478.0 nm, stable *Q*-switching with a maximum average power of 583.7 mW was achieved with a slope efficiency of 15.2% relative to the launched 1981 nm pump power. Further power scaling is mainly limited by the available 1981 nm pump power. The corresponding pulse width, repetition rate, and pulse energy are 1.18 μs, 71.43 kHz, and 7.54 μJ, respectively. By rotating the grating, the *Q*-switching can be continuously tuned in the region of 3.4–3.7 μm. To the best of our knowledge, this is the first pulsed rare-earth-doped fiber laser tunable in the region beyond 3.4 μm.

https://doi.org/10.1364/PRJ.7.001106

1. INTRODUCTION

As a valuable spectral region, mid-infrared 2–20 μm contains strong characteristic vibrational transitions of a series of important molecules and two atmospheric transmission windows (i.e., 3–5 μm and 8–13 μm) [1]. Motivated by growing demands in the fields of medicine, industry, security, etc., lasers in this spectral region have attracted increased interest in the last several decades. Nowadays, many laser technologies are serving this range, e.g., optical parametric oscillator [2], quantum cascade laser [3], and doped insulator laser [4]. The fiber laser, as one of the doped insulator lasers [5], has been strongly developed because of its great power scalability, near-diffraction-limited beam quality, compact and robust structure, and recently, towards the mid-infrared region [6]. Among them, the ~2.8 μm transition ($^4I_{11/2} \rightarrow {}^4I_{13/2}$) in Er^{3+}-doped ZrF_4 fiber laser was paid most attention to owing to the mature 976 nm diode pumping technique and efficient energy transfer upconversion (ETU), enabling lasing beyond the Stokes limit [7]. The continuous wave (CW) laser at 2.82 μm was scaled to 40.6 W power recently by Aydin *et al.* [8], and the power was further boosted to a record 65 W under quasi-continuous wave (QCW) by Newburgh *et al.* very recently [9]. Based on this platform, the comparative efforts on pulse operation by *Q* switching, gain switching, and mode locking have been widely reported [10]. For example, Tokita *et al.* presented an actively *Q*-switched Er^{3+}-doped ZrF_4 fiber laser at 2.8 μm, giving an average power of up to 12 W and a pulse energy of 100 μJ at the repetition rate of 120 kHz [11]. In the same way, Lamrini *et al.* scaled the pulse energy to 560 μJ at the repetition rate of 1 kHz [12]. Wei *et al.* utilized a Fe^{2+}:ZnSe crystal to realize high-power passive *Q* switching, tunable in the range of 2762.5–2852.5 nm, where the maximum average power of 5.16 W and pulse energy of 27.7 μJ were achieved at 2.81 μm [13]. Paradis *et al.* demonstrated a gain-switched Er^{3+}-doped ZrF_4 fiber laser at 2.826 μm with an average power of 11.2 W and a pulse energy of 80 μJ [14]. Duval *et al.* reported the first femtosecond-level mode-locked Er^{3+}-doped ZrF_4 fiber laser in a ring cavity using nonlinear polarization rotation [15], yielding a peak power of 3.5 kW with a pulse width of 207 fs. Because of the longer emission band around 3 μm, $^5I_6 \rightarrow {}^5I_7$ and $^6H_{13/2} \rightarrow {}^6H_{15/2}$ transitions in Ho^{3+}- and Dy^{3+}-doped ZrF_4 fibers have also received much attention [16–25]. So far, their CW and pulsed versions have covered the broad range of 2.7–3.4 μm, with some shining results, such as a record peak power of 37 kW from a mid-infrared fiber oscillator [18], and a record tuning range of ~600 nm (2.8–3.4 μm) from a rare-earth-doped fiber oscillator [21].

At longer wavelengths of ~3.5 μm, Többen *et al.* demonstrated lasing from an Er^{3+}-doped ZrF_4 fiber laser based on $^4F_{9/2} \rightarrow {}^4I_{9/2}$ transition pumped at 653 nm at a temperature

of 77 K as early as 1991 [26]. Poor performance due mainly to the ions bottlenecking issue caused by the long-lived excited states, however, limited its development in the following several decades. As a result, its applications in polymer processing (e.g., methyl methacrylate, polypropylene, polyethylene) [27] and gas monitoring (e.g., methane, propane, formaldehyde) [28] are also blocked. Until 2014, efficient emission potential of this transition was unlocked by Henderson-Sapir *et al.* for the first time using the proposed dual-wavelength pumping (DWP) (985 nm + 1983 nm) concept, where the ions bottlenecking issue was solved [29]. And beyond 200 mW, CW lasers around 3.5 μm with an optical-to-optical efficiency of 16% were reached at room temperature [29]. Subsequently, Henderson-Sapir and colleagues realized ~450 nm (3.33–3.78 μm) CW wavelength tuning [30], and Maes *et al.* scaled the average power to 5.6 W at 3.55 μm [31]. Meanwhile, the theoretical analyses were also made to deeply understand the dynamics of this system [32–34]. Along with the success in CW, its pulsed versions were constructed owing to higher peak power and pulse energy. Jobin *et al.* presented the first gain-switched DWP Er^{3+}-doped ZrF_4 fiber laser at 3.55 μm [35]. A high peak power of up to 204 W and a pulse energy of 6.83 μJ were achieved at the repetition rate of 15 kHz [35]. Then we scaled the average power to 1.04 W by a factor of 10 by using microsecond-scale pulse pumping to relieve power quenching during one pump pulse [36]. In comparison to gain switching, *Q* switching just needs a cost-effective CW pump source while avoiding the possible relaxation oscillation spikes. And the availability of all-fiber passive modulators using the emerging low-dimensional materials also pushed the progress of *Q* switching technique. In fact, self-*Q*-switching behavior was observed by Henderson-Sapir *et al.* in their first demonstration of DWP ~3.5 μm emission [37]. Then they numerically predicted the feasibility of active *Q* switching in such a system [38] and experimentally realized actively *Q*-switched pulses using an acousto-optic modulator, yielding a peak power of 14.5 W and a pulse energy of 7.8 μJ [39]. Qin *et al.* used black phosphorus (BP) to present passive *Q* switching and mode locking from a DWP Er^{3+}-doped ZrF_4 fiber laser at ~3.5 μm [40]. However, the low damage threshold of BP led to the limited average power of 120 mW and pulse energy of 1.8 μJ [40]. Low-dimensional materials represented by BP have been serving pulsed fiber lasers as saturable absorbers (SAs) from the visible to the mid-infrared region for almost one decade owing to their broadband feature [41,42]. Although overcoming the narrow operation band of the traditional semiconductor SA mirror, they most contribute to quite moderate output due to their low damage thresholds.

Fe^{2+}:ZnSe is another alternative SA applicable in the mid-infrared region as a result of its strong absorption in the range of 2.5–4.5 μm. More importantly, it has a damage threshold of up to ~2 J/cm^2 with a small saturation, suitable for powerful and energetic *Q* switching. To date, ~2.8 μm Er^{3+}- and ~2.9 μm Ho^{3+}-doped ZrF_4 fiber lasers *Q*-switched by Fe^{2+}:ZnSe have been widely reported [13,43–46], of which output scaling was limited by pump power or damaged fiber ends instead of Fe^{2+}:ZnSe itself. At wavelengths beyond 3 μm, although the absorption decreases with the wavelength [47], which implies an increased initial transmission, and hence a decreased modulation depth for a certain Fe^{2+}:ZnSe crystal, it should still be effective as an SA at <4.5 μm in principle. However, no relative efforts have been reported so far, to the best of our knowledge.

In this paper, we extend the Fe^{2+}:ZnSe-based *Q*-switching technique to operate in a tunable region of 3.4–3.7 μm, based on a DWP (976 nm + 1981 nm) Er^{3+}-doped ZrF_4 fiber laser. This is the first tunable pulsed rare-earth-doped fiber laser in this band. Attributable to the high damage threshold of the Fe^{2+}:ZnSe SA, the output average power and pulse energy of passive *Q* switching are significantly scaled to 583.7 mW and 9.07 μJ (not simultaneously), only limited by the available pump power at 1981 nm. The output characteristics, including pulse width, repetition rate, average/peak power, and pulse energy with the varied pump power and operation wavelength, were also studied.

2. EXPERIMENTAL SETUP

Figure 1 shows the experimental setup of our constructed tunable passively *Q*-switched Er^{3+}-doped ZrF_4 fiber laser based on a Fe^{2+}:ZnSe crystal around 3.5 μm. The pump unit includes two laser sources, one of which is a commercial 976 nm laser diode (LD) (BWT, China) with a fiber pigtail [core/numerical aperture (NA): 105/0.22] yielding a maximum output power of 30 W; the other is an in-house CW 1981 nm Tm^{3+}-doped fiber oscillator whose cavity is formed by a pair of fiber Bragg gratings (FBGs) with an SMF-28e fiber pigtail yielding a maximum output power of 8 W. The 976 nm laser is collimated using an objective lens (L1, Melles Griot) with a focal length of 10 mm, and the 1981 nm laser is collimated using an aspheric mirror (L2, C240TME-C, Thorlabs) with a focal length of 8 mm. They are combined using a dichroic mirror (DM1, DMSP1500, Thorlabs) placed at an angle of 45° relative to the light axis and then launched into the cladding and core of the gain fiber using an objective lens (L3, LFO-5-6, Innovation Photonics) (transmission 90% at 1981 nm, 70%

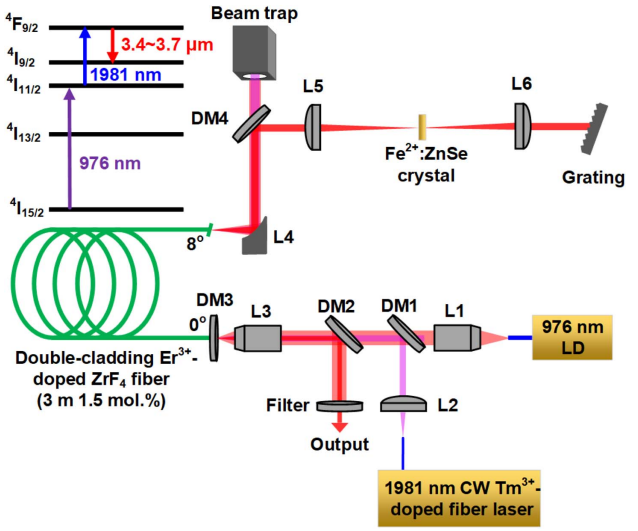

Fig. 1. Experimental setup of the Fe^{2+}:ZnSe crystal passively *Q*-switched Er^{3+}-doped ZrF_4 fiber laser tunable around 3.5 μm. DM1–DM4, four DMs; L1–L6, six lenses.

at 976 nm, and 95% at ~3.5 μm) with an efficiency of 76% and 86%, respectively. A dichroic mirror (DM2, transmission 97% at 1981 nm, 85% at 976 nm, and reflection >98% at ~3.5 μm) is placed between L3 and DM1 to steer the laser from the $^4F_{9/2} \rightarrow {}^4I_{9/2}$ transition (see the inset of Fig. 1). After that, a commercial bandpass filter (Thorlabs, FB3500-500) is used to purify the ~3.5 μm laser. The gain medium is a piece of 3 m double-cladding Er^{3+}-doped ZrF_4 fiber (Le Verre Fluoré, France) with a dopant concentration of 1.5 mol.%. The core has a diameter of 16.5 μm with an NA of 0.15, and the inner cladding has a diameter of 260 μm with two parallel flats separated by 240 μm. Its outer cladding is a low-index fluoroacrylate polymer with a diameter of 290 μm. The fiber end close to the pump is perpendicularly cleaved and butted against a dichroic mirror (DM3, transmission 95% at 1981 nm, 96% at 976 nm, and reflection ~60% at ~3.5 μm) acting as the cavity feedback and output coupler. The other fiber end is cleaved at an angle of 8° to suppress ~2.8 μm oscillation and ~3.5 μm parasitic laser. The ~3.5 μm laser from the angle-cleaved fiber end is collimated using an off-axis parabolic reflector (L4, Thorlabs, MPD00M9-P01) with a focal length of 15 mm to avoid focal position shift over the entire tuning range. A dichroic mirror (DM4), the same as DM2, is placed at an angle of 45° to reflect the ~3.5 μm laser while the transmitted residual 976 and 1981 nm laser is collected using a beam trap. The reflected laser is resonated by a plane-ruled grating (Thorlabs, 450 lines per mm, blaze wavelength $\lambda_B = 3.1$ μm, blaze angle $\theta_B = 32°$) in a Littrow configuration. The wavelength can be tuned by rotating the grating. A confocal scheme including two commercial uncoated CaF_2 plano–convex lenses (L5, L6, Thorlabs, LA5763) with a focal length of 50 mm is placed between the grating and DM3. The Fe^{2+}:ZnSe crystal with a size of 6.7 mm × 6.7 mm × 1.6 mm and a Fe^{2+} doping concentration of 0.9×10^{18} cm^{-3} (provided by the manufacturer) is mounted and connected with a one-dimensional platform, and then inserted into the confocal scheme and carefully adjusted near the focal point. Its initial transmission at ~3.5 μm was measured to be ~80% using a CW laser source with a low average power. Due to lack of a high energy pulsed source at ~3.5 μm, its saturable absorption parameters were not measured. Nevertheless, its modulation depth could be roughly estimated to be close to ~20% considering the small unsaturation loss [48]. Notice that no heat management was imposed on it. Although the relatively long upper state lifetime of 370 ± 25 ns for Fe^{2+}:ZnSe at room temperature [47] makes it difficult to realize megahertz-level high repetition rate Q-switching, this is in turn beneficial for higher pulse energy owing to lower photon loss caused by the SA. In our experiment, the position of the Fe^{2+}:ZnSe crystal needs to be optimized to maximize the output power while producing stable Q-switched pulses. The laser power was recorded using a high-resolution thermal power sensor (Thorlabs, S405C), the temporal pulses were captured using an InAs detector (Judson J12D) with a response time of 2 ns connected with a 500 MHz bandwidth digital oscilloscope, and the optical spectrum was measured using a monochromator (Princeton Instrument Acton SP2300). Note that the laser powers mentioned in this paper are all corrected.

3. RESULTS

First, we adjusted the launched 1981 nm pump power to the available maximum 5.25 W and then increased the launched 976 nm pump power to 2.47 W while rotating the grating to

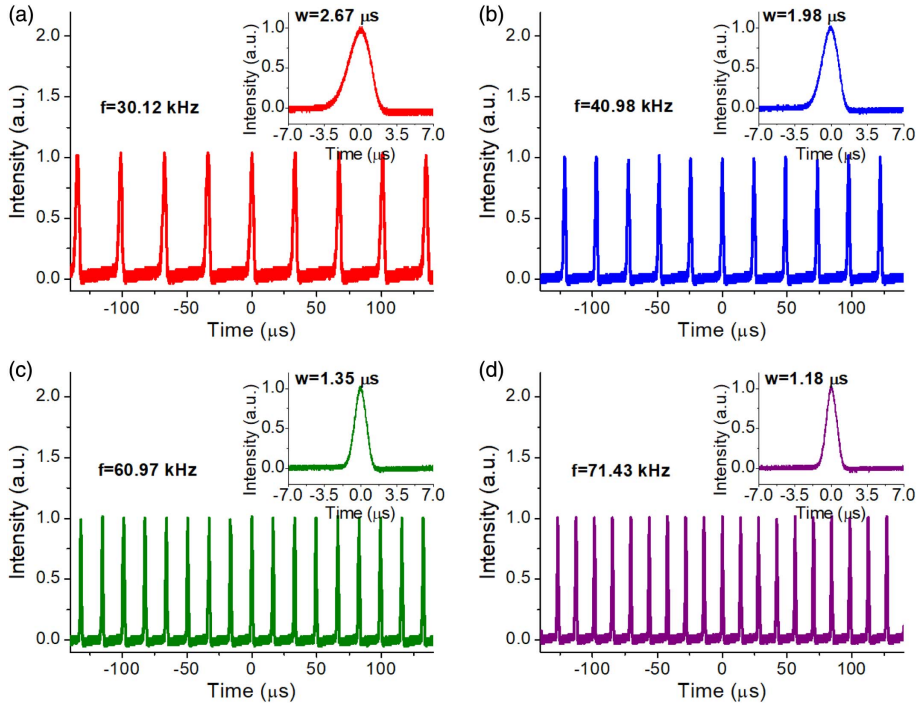

Fig. 2. Q-switched pulse train and single pulse waveform (inset) at different launched 1981 nm pump powers. (a) 2.24 W, (b) 2.78 W, (c) 4.19 W, and (d) 5.25 W. ($P_{\text{launched 976 nm}} = 2.47$ W.)

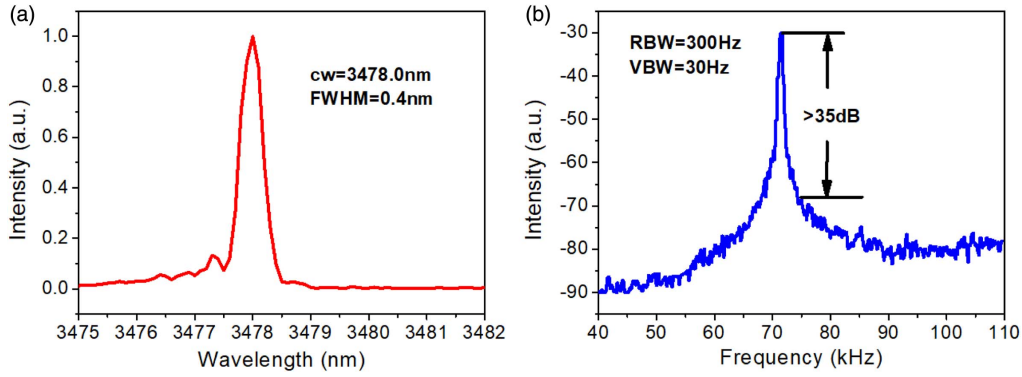

Fig. 3. (a) Optical and (b) RF spectra at the launched 1981 nm pump power of 5.25 W. ($P_{\text{launched 976 nm}} = 2.47$ W.)

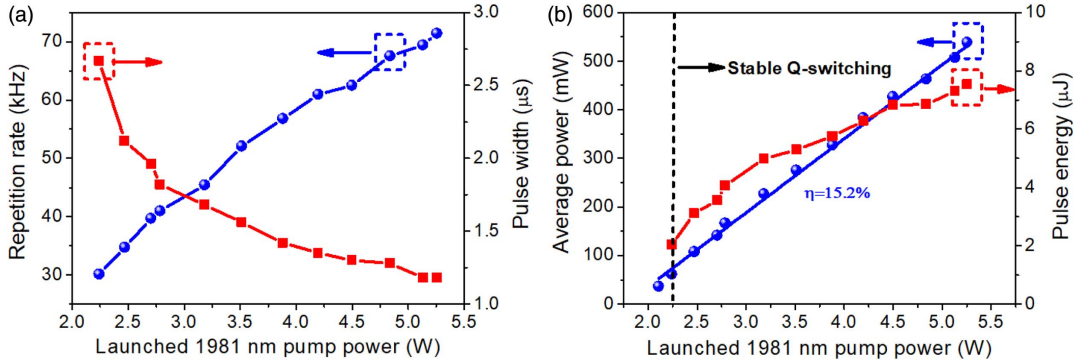

Fig. 4. (a) Repetition rate and pulse width; (b) average power and pulse energy as functions of the launched 1981 nm pump power. ($P_{\text{launched 976 nm}} = 2.47$ W.)

maximize the ~3.5 μm output power. After that, the laser output characteristics as the varied launched 1981 nm pump power were recorded, keeping the launched 976 nm pump power at 2.47 W and the position of the grating unchanged.

Increasing the launched 1981 nm pump power to 2.10 W, a Q switching sign with quite low amplitudes and serious fluctuations first appeared. Further increasing the pump to 2.24 W, stable Q-switched pulses were achieved as displayed in Fig. 2(a), yielding a repetition rate of 30.12 kHz and a pulse width of 2.67 μs. This stable Q-switching regime could be maintained until the maximum launched 1981 nm pump power of 5.25 W, as shown in Fig. 2(d), giving a low amplitude fluctuation of ±1.4%. The temporal behaviors at the middle 1981 nm pump powers of 2.78 and 4.19 W were also recorded, as shown in Figs. 2(b) and 2(c), respectively. At the maximum 1981 nm pump power, the optical and RF spectra were measured, as shown in Figs. 3(a) and 3(b), respectively. It is seen that only one strong spectral peak centered at 3478.0 nm with a narrow FWHM of 0.4 nm is observed, different from the several spectral lines in free-running cases [36,39,40]. This suggests that the plane-ruled grating in our case takes effect. The signal-to-noise ratio (SNR) of >35 dB for the fundamental frequency is also located within the typical range of stable passive Q switching [43–46].

Figure 4(a) plots the variations of repetition rate and pulse width as the 1981 nm pump power was launched. It is observed that both undergo the same variation trend as standard passive Q switching. At the maximum launched 1981 nm pump power, the largest repetition rate of 71.43 kHz and shortest pulse width of 1.18 μs were achieved, while the average output power reached the maximum 583.7 mW, with a slope efficiency of 15.2% relative to the launched 1981 nm pump power, as shown in Fig. 4(b). The corresponding pulse energy was calculated to be 7.54 μJ. Further power and energy scaling was limited by the available 1981 nm pump power.

Then wavelength tuning of the Q-switched fiber laser was performed. Figure 5 displays the recorded optical spectra and

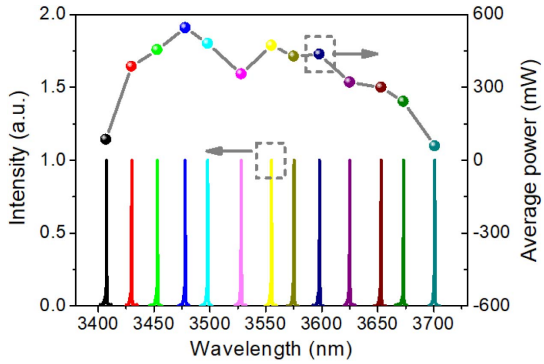

Fig. 5. Optical spectrum and output average power with the tuned wavelength. ($P_{\text{launched 1981 nm}} = 5.25$ W, $P_{\text{launched 976 nm}} = 2.47$ W.)

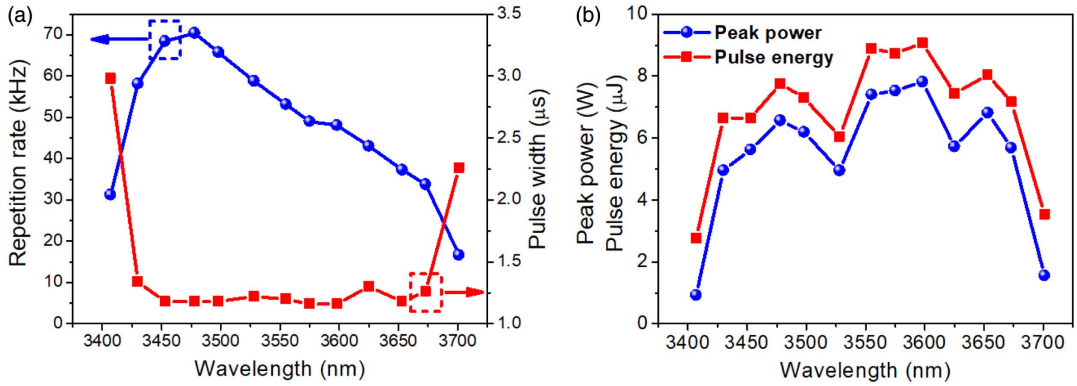

Fig. 6. (a) Repetition rate and pulse width; (b) peak power and pulse energy as functions of the tuned wavelength. ($P_{\text{launched 1981 nm}} = 5.25$ W, $P_{\text{launched 976 nm}} = 2.47$ W.)

corresponding average output powers when rotating the grating at the launched 1981 nm pump power of 5.25 W. The wavelength of stable Q-switched pulses can be continuously tuned within a ~300 nm range of 3407.2–3701.1 nm. The average power increases first and decreases with tuning towards the long wavelength, in agreement with the gain spectrum of this transition [29]. To identify the factors limiting further extension of the tuning range, considering that it is much narrower than the ~450 nm CW tuning range of 3330–3780 nm [30], we removed the confocal scheme and Fe^{2+}:ZnSe crystal to reduce the intracavity insertion loss. As a result, only a moderately extended ~345 nm CW tuning range of 3385.2–3730.6 nm was obtained. It suggests that the tuning range extension in our system is mainly limited by the available 1981 nm pump power, for which it is quite difficult to make gains at the wavelengths outside the range reaching laser thresholds.

Figure 6(a) shows the variations of repetition rate and pulse width with the tuned wavelength. With tuning from 3407.2 to 3701.1 nm, the repetition rate changes between 16.67 and 71.43 kHz, with a similar variation trend to that of the average power shown in Fig. 5. This is because higher intracavity laser power leads to faster bleaching of the Fe^{2+}:ZnSe crystal, thus to a larger repetition rate, while the pulse width varies between 2.98 and 1.16 μs. Over this wavelength range, the varied pulse peak powers and energies were also recorded, as shown in Fig. 6(b). Almost the same variation trends as that of the average power are observed. At the tuned wavelength of 3598.3 nm, the maximum peak power of 7.82 W and pulse energy of 9.07 μJ were achieved.

4. CONCLUSION

In summary, we have presented a tunable passively Q-switched DWP Er^{3+}-doped ZrF_4 fiber laser around 3.5 μm using a Fe^{2+}:ZnSe crystal as the SA and a plane-ruled grating in a Littrow configuration as the tuning element. To the best of our knowledge, this is also the first tunable pulsed laser based on rare-earth-doped fibers at ~3.5 μm. At the tuned wavelength of 3478.0 nm, stable Q-switched pulses could yield a maximum average power of 583.7 mW with the corresponding pulse width, repetition rate, and pulse energy of 1.18 μs, 71.43 kHz, and 7.54 μJ, respectively. Further power scaling is only limited by the available 1981 nm pump power. By rotating the grating, the wavelength of Q-switched pulses could be tuned continuously from 3407.2 to 3701.1 nm; further extension is mainly limited by the available 1981 nm pump power. The work in this paper has extended the Fe^{2+}:ZnSe-based Q-switching technique to operate in the longest 3.5 μm band for the first time, to the best of our knowledge. In the next step, power scaling will be continued, aided by the advantageous high damage threshold of the Fe^{2+}:ZnSe crystal. Moreover, we will also attempt to utilize the Fe^{2+}:ZnSe crystal to realize passive mode locking at ~3.5 μm, considering its success in a 2.8 μm mode-locked Er^{3+}-doped ZBLAN fiber laser [49]. Specifically, we plan to further increase the intracavity intensity based on a ring cavity while improving the SA initial transmission by reducing its doping concentration and thickness to make the CW mode-locking condition easier.

Funding. National Natural Science Foundation of China (NSFC) (61722503, 61421002, 61435003); Open Fund of Science and Technology on Solid-State Laser Laboratory; Joint Fund of Ministry of Education for Equipment Pre-Research (6141A02033411); Field Funding for Equipment Pre-Research (1114180106A).

Acknowledgment. H. Y. Luo and J. Yang contributed equally to this work. H. Y. Luo and J. F. Li designed the experiment. H. Y. Luo prepared the paper and discussed it with J. F. Li. J. Yang built up the system and finished the measurements with H. Y. Luo. Y. Liu supervised the project.

REFERENCES

1. A. Hoffman and C. Gmachl, "Extending opportunities," Nat. Photonics **6**, 407 (2012).
2. N. Y. Kostyukova, A. A. Boyko, V. Badikov, D. Badikov, G. Shevyrdyaeva, V. Panyutin, G. M. Marchev, D. B. Kolker, and V. Petrov, "Widely tunable in the mid-IR $BaGa_4Se_7$ optical parametric oscillator pumped at 1064 nm," Opt. Lett. **41**, 3667–3670 (2016).
3. Y. Yao, A. J. Hoffman, and C. F. Gmachl, "Mid-infrared quantum cascade lasers," Nat. Photonics **6**, 432–439 (2012).
4. A. Godard, "Infrared (2–12 μm) solid-state laser sources: a review," C. R. Physique **8**, 1100–1128 (2007).
5. https://www.rp-photonics.com/mid_infrared_laser_sources.html.

6. S. D. Jackson, "Towards high-power mid-infrared emission from a fiber laser," Nat. Photonics **6**, 423–431 (2012).
7. D. Faucher, M. Bernier, G. Androz, N. Caron, and R. Vallée, "20 W passively cooled single-mode all-fiber laser at 2.8 μm," Opt. Lett. **36**, 1104–1106 (2011).
8. Y. O. Aydin, V. Fortin, R. Vallée, and M. Bernier, "Towards power scaling of 2.8 μm fiber lasers," Opt. Lett. **43**, 4542–4545 (2018).
9. G. A. Newburgh, M. Dubinskii, J. Zhang, and W. Lu, "A power scaled diode cladding pumped 2.8 μm Er:ZBLAN fiber laser," Proc. SPIE **10981**, 1098107 (2019).
10. X. Zhu, G. Zhu, C. Wei, L. V. Kotov, J. Wang, M. Tong, R. A. Norwood, and N. Peyghambarian, "Pulsed fluoride fiber lasers at 3 μm [invited]," J. Opt. Soc. Am. B **34**, A15–A28 (2017).
11. S. Tokita, M. Murakami, S. Shimizu, M. Hashida, and S. Sakabe, "12 W *Q*-switched Er:ZBLAN fiber laser at 2.8 μm," Opt. Lett. **36**, 2812–2814 (2011).
12. S. Lamrini, K. Scholle, M. Schäfer, J. Ward, M. Francis, M. Farries, S. Sujecki, T. Benson, A. Seddon, A. Oladeji, B. Napier, and P. Fuhrberg, "High-energy *Q*-switched Er:ZBLAN fibre laser at 2.79 μm," in *Conference on Lasers and Electro-Optics/European Quantum Electronics Conference* (2015), paper CJ_7_2.
13. C. Wei, H. Zhang, H. Shi, K. Konynenbelt, H. Luo, and Y. Liu, "Over 5-W passively Q-switched mid-infrared fiber laser with a wide continuous wavelength tuning range," IEEE Photon. Technol. Lett. **29**, 881–884 (2017).
14. P. Paradis, V. Fortin, Y. O. Aydin, R. Vallée, and M. Bernier, "10 W-level gain-switched all-fiber laser at 2.8 μm," Opt. Lett. **43**, 3196–3199 (2018).
15. S. Duval, M. Bernier, V. Fortin, J. Genest, M. Piché, and R. Vallée, "Femtosecond fiber lasers reach the mid-infrared," Optica **2**, 623–626 (2015).
16. J. F. Li, D. D. Hudson, and S. D. Jackson, "High-power diode-pumped fiber laser operating at 3 μm," Opt. Lett. **36**, 3642–3644 (2011).
17. S. Crawford, D. D. Hudson, and S. D. Jackson, "High-power broadly tunable 3-μm fiber laser for the measurement of optical fiber loss," IEEE Photon. J. **7**, 1502309 (2015).
18. S. Antipov, D. D. Hudson, A. Fuerbach, and S. D. Jackson, "High-power mid-infrared femtosecond fiber laser in the water vapor transmission window," Optica **3**, 1373–1376 (2016).
19. H. Y. Luo, J. F. Li, Y. C. Hai, X. Lai, and Y. Liu, "State-switchable and wavelength-tunable gain-switched mid-infrared fiber laser in the wavelength region around 2.94 μm," Opt. Express **26**, 63–79 (2018).
20. H. Y. Luo, X. L. Tian, Y. Gai, R. F. Wei, J. F. Li, J. Qiu, and Y. Liu, "Antimonene: a long-term stable two-dimensional saturable absorption material under ambient conditions for the mid-infrared spectral region," Photon. Res. **6**, 900–907 (2018).
21. M. R. Majewski, R. I. Woodward, and S. D. Jackson, "Dysprosium-doped ZBLAN fiber laser tunable from 2.8 μm to 3.4 μm, pumped at 1.7 μm," Opt. Lett. **43**, 971–974 (2018).
22. R. I. Woodward, M. R. Majewski, and S. D. Jackson, "Mode-locked dysprosium fiber laser: picosecond pulse generation from 2.97 to 3.30 μm," APL Photon. **3**, 116106 (2018).
23. Y. Wang, F. Jobin, S. Duval, V. Fortin, P. Laporta, M. Bernier, G. Galzerano, and R. Vallée, "Ultrafast Dy^{3+}:fluoride fiber laser beyond 3 μm," Opt. Lett. **44**, 395–398 (2019).
24. R. I. Woodward, M. R. Majewski, N. Macadam, G. Hu, T. Albrow-Owen, T. Hasan, and S. D. Jackson, "*Q*-switched Dy:ZBLAN fiber lasers beyond 3 μm: comparison of pulse generation using acousto-optic modulation and inkjet-printed black phosphorus," Opt. Express **27**, 15032–15045 (2019).
25. H. Y. Luo, J. Yang, Y. Gao, Y. Xu, X. H. Li, and Y. Liu, "Tunable passively *Q*-switched Dy^{3+}-doped fiber laser from 2.71 to 3.08 μm using PbS nanoparticles," Opt. Lett. **44**, 2322–2325 (2019).
26. H. Többen, "CW lasing at 3.45 μm in erbium-doped fluorozirconate fibres," Frequenz **45**, 250–252 (1991).
27. C. Frayssinous, V. Fortin, J.-P. Bérubé, A. Fraser, and R. Vallée, "Resonant polymer ablation using a compact 3.44 μm fiber laser," J. Mater. Process. Technol. **252**, 813–820 (2018).
28. A. E. Klingbeil, J. B. Jeffries, and R. K. Hanson, "Temperature- and pressure-dependent absorption cross sections of gaseous hydrocarbons at 3.39 μm," Meas. Sci. Technol. **17**, 1950–1957 (2006).
29. O. Henderson-Sapir, J. Munch, and D. J. Ottaway, "Mid-infrared fiber lasers at and beyond 3.5 μm using dual wavelength pumping," Opt. Lett. **39**, 493–496 (2014).
30. O. Henderson-Sapir, S. D. Jackson, and D. Ottaway, "Versatile and widely tunable mid-infrared erbium doped ZBLAN fiber laser," Opt. Lett. **41**, 1676–1679 (2016).
31. F. Maes, V. Fortin, M. Bernier, and R. Vallée, "5.6 W monolithic fiber laser at 3.55 μm," Opt. Lett. **42**, 2054–2057 (2017).
32. O. Henderson-Sapir, J. Munch, and D. J. Ottaway, "New energy-transfer upconversion process in Er^{3+}:ZBLAN mid-infrared fiber lasers," Opt. Express **24**, 6869–6883 (2016).
33. A. Malouf, O. Henderson-Sapir, M. Gorjan, and D. J. Ottaway, "Numerical modeling of 3.5 μm dual-wavelength pumped erbium doped mid-infrared fiber lasers," IEEE J. Quantum Electron. **52**, 1600412 (2016).
34. F. Maes, V. Fortin, M. Bernier, and R. Vallée, "Quenching of 3.4 μm dual-wavelength pumped erbium doped fiber lasers," IEEE J. Quantum Electron. **53**, 1600208 (2017).
35. F. Jobin, V. Fortin, F. Maes, M. Bernier, and R. Vallée, "Gain-switched fiber laser at 3.55 μm," Opt. Lett. **43**, 1770–1773 (2018).
36. H. Y. Luo, J. Yang, F. Liu, Z. Hu, Y. Xu, F. Yan, H. L. Peng, F. Ouellette, J. F. Li, and Y. Liu, "Watt-level gain-switched fiber laser at 3.46 μm," Opt. Express **27**, 1367–1375 (2019).
37. O. Henderson-Sapir, J. Munch, and D. J. Ottaway, "A higher power 3.5 μm fiber laser," in *Advanced Solid State Lasers* (2014), paper ATu1A.3.
38. O. Henderson-Sapir, A. Malouf, N. Bawden, J. Munch, S. D. Jackson, and D. J. Ottaway, "Recent advances in 3.5 μm erbium doped mid-infrared fiber lasers," IEEE J. Sel. Top. Quantum Electron. **23**, 6–14 (2016).
39. N. Bawden, H. Matsukuma, O. Henderson-Sapir, E. Klantsataya, S. Tokita, and D. J. Ottaway, "Actively *Q*-switched dual-wavelength pumped Er^{3+}:ZBLAN fiber laser at 3.47 μm," Opt. Lett. **43**, 2724–2727 (2018).
40. Z. Qin, T. Hai, G. Xie, J. Ma, P. Yuan, L. Qian, L. Li, L. Zhao, and D. Shen, "Black phosphorus *Q*-switched and mode-locked mid-infrared Er:ZBLAN fiber laser at 3.5 μm wavelength," Opt. Express **26**, 8224–8231 (2018).
41. B. Guo, "2D noncarbon materials-based nonlinear optical devices for ultrafast photonics [invited]," Chin. Opt. Lett. **16**, 020004 (2018).
42. K. Wu, B. H. Chen, X. Y. Zhang, S. F. Zhang, C. S. Guo, C. Li, P. S. Xiao, J. Wang, L. J. Zhou, W. W. Zou, and J. P. Chen, "High-performance mode-locked and *Q*-switched fiber lasers based on novel 2D materials of topological insulators, transition metal dichalcogenides and black phosphorus: review and perspective (invited)," Opt. Commun. **406**, 214–229 (2018).
43. C. Wei, X. S. Zhu, R. A. Norwood, and N. Peyghambarian, "Passively *Q*-switched 2.8-μm nanosecond fiber laser," IEEE Photon. Technol. Lett. **24**, 1741–1744 (2012).
44. G. W. Zhu, X. S. Zhu, K. Balakrishnan, R. A. Norwood, and N. Peyghambarian, "Fe^{2+}:ZnSe and graphene *Q*-switched singly Ho^{3+}-doped ZBLAN fiber lasers at 3 μm," Opt. Mater. Express **3**, 1365–1377 (2013).
45. T. Zhang, G. Y. Feng, H. Zhang, X. H. Yang, S. Y. Dai, and S. H. Zhou, "2.78 μm passively *Q*-switched Er^{3+}-doped ZBLAN fiber laser based on PLD-Fe^{2+}:ZnSe film," Laser Phys. Lett. **13**, 075102 (2016).
46. S. G. Ning, G. Y. Feng, H. Zhang, W. Zhang, S. Y. Dai, Y. Xiao, W. Li, X. X. Chen, and X. H. Zhou, "Fabrication of Fe^{2+}:ZnSe nanocrystals and application for a passively *Q*-switched fiber laser," Opt. Mater. Express **8**, 865–874 (2018).
47. V. V. Fedorov, S. B. Mirov, A. Gallian, D. V. Badikov, M. P. Frolov, Y. V. Korostelin, V. I. Kozlovsky, A. I. Landman, Y. P. Podmar'kov, V. A. Akimov, and A. A. Voronov, "3.77–5.05 μm tunable solid-state lasers based on Fe^{2+}-doped ZnSe crystals operating at low and room temperatures," IEEE J. Quantum Electron. **42**, 907–917 (2006).
48. https://www.ipgphotonics.com/en/88/Widget/Passive+Q-switch+Fe_ZnS+and+Fe_ZnSe+Datasheet.pdf.
49. C. Wei, X. S. Zhu, R. A. Norwood, and N. Peyghambarian, "Passively continuous-wave mode-locked Er^{3+}-doped ZBLAN fiber laser at 2.8 μm," Opt. Lett. **37**, 3849–3851 (2012).